Korean J. Chem. Eng., **21**(5), 1053-1061 (2004)

Optimal Design of Multi-stage Porous Plate Collection System

Seok-Jun Yoa†, Yong-Soo Cho, Jun-Ho Kim, Il-Kyu Kim and Jea-Keun Lee

Department of Environmental Engineering, Pukyong National University, 599-1, Daeyon-Dong, Nam-Gu, Pusan 608-737, Korea
(*Received 25 March 2004 • accepted 24 June 2004*)

Abstract–The main objective of this study was to investigate the optimal design parameters of a multi-stage porous plate system, numerically and experimentally. Characteristics of pressure drop and collection efficiency are analyzed with the operation parameters such as the stage number, plate interval, hole diameter and system inlet velocity, etc. In the results, pressure drops of a 5 stage system [2, 2, 3, 2, 2 mm] at $v_{s,in}$=1.0, 1.2 m/s are shown as 296, 428 mmH_2O by the numerical simulation and 259, 399 mmH_2O in the experiment. For 5 stage [2, 2, 3, 2, 2 mm] and $v_{s,in}$=1.0 m/s, the overall collection efficiencies with the plate interval 4, 10, 15 mm are estimated as 99.5, 96.0, 92.8% computationally and 97.9, 89.2, 85.3%, showing slightly lower efficiency compared to the numerical results due to the particle rescattering effect, experimentally.

Key words: Multi-Stage Porous Plate, Collection Efficiency, Pressure Drop, Stage Number, Plate Interval

INTRODUCTION

The recent tightening of emission control laws for air pollution has necessitated the exchange and modification of conventional industrial air pollution control equipment.

ESP and fabric bag filters widely used up to now have had some problems in spite of their many merits, such as high collection efficiency [Robinson, 1971; Oglesby et al., 1978]. ESP can treat high volumetric flow rates without a serious pressure drop, and has the advantage of easy maintenance and repair, but it has the disadvantage of equipment scale enlargement for the large collection area in order to maintain high efficiency over 99% [Croom, 1994; Yoa et al., 2001; Frederick, 1961]. The fabric bag filter has been recognized as the most popular control equipment with high collection efficiency and wide field application, while it has significant problems such as the enlargement of equipment scale and excessive pressure drop by the accumulation of dust, including vapor due to the hot gas condensation on the filter surface [Ohtsuk, 1986].

Thus, it is absolutely necessary to develop advanced control equipment based on a new concept of collection system to overcome the above problems. To do that, the present study is focused on the development of a multi-stage porous plate system which can show simplicity of design (smaller scale), high collection efficiency and high flow rates by the combination of impaction and turbulent diffusion mechanism, etc. without filter dependency. In the present collection system composed of a multiple array of porous plates, the impinging jet flows of high speed through the porous plate holes in a two-phase system accompanying the dust particle induce a strong inertial effect toward the next staggered porous plate (Fig. 2). Also, smaller particles are mainly collected on the back surface of a prior porous plate by the turbulent diffusion effect in a recirculation region formed between the adjacent porous plates [Daniel et al., 1998; Novick et al., 1987; Benjamin et al., 1995].

Finally, it is important to investigate the main parameters for the optimal design of the multi-stage porous plate system by carrying out a numerical and experimental analysis with various system parameters such as stage number, system inlet velocity, hole diameter and plate to plate distance, etc. in the present study.

†To whom correspondence should be addressed.
E-mail: sjyoa@pknu.ac.kr

EXPERIMENTAL AND NUMERICAL ANALYSIS

1. Experimental Apparatus and Procedure

The experimental system is constructed with main body (porous plate), particle generator, duct line, I.D. fan and measuring part. The gas velocity, pressure drop and collection efficiency are detected by Anemometer (model 6621, Kanomax LTD.), Micromanometer (FCO 332, Furness Controls LTD.) and APS(Aerodynamic Particle Sizer, TSI Inc.), respectively. The layout of the experimental apparatus for this study is shown in Fig. 1.

The dimensions of the porous plate are 2 mm thickness, 170 mm height and 60 mm width. For the analysis of pressure drop and collection efficiency characteristics, an experiment was performed with major parameters such as stage number, system inlet velocity and hole diameter, etc. as shown in Fig. 2. For the increase of the impaction effect, hole positions were staggered with plate arrangement. Plate surface is coated with grease for minimization of the slip effect [Bernard et al., 1998; Chang et al., 1999]. Table 1 shows the hole velocity (jet flow velocity through a hole) with hole diameter.

2. Numerical Method

The physical configuration for the numerical simulation of the multi-stage porous plate system depicts the porous plate arrangement by the same interval of 2 or 3 mm diameter holes intercoupled iteratively on the adjacent plates (front and back stage) with each other as in Fig. 3. As shown in Figs. 3 and 4, the computational domain includes the several modules of rectangular shape, and computationally, only one module involving the 4 minimum units is utilized by geometric symmetry to save computational time. The FLUENT code was used for the present numerical simulation of gaseous flow and particle transport. The SIMPLE algorithm and the k-ε model were used for evaluating the turbulent flow field. A 3D unstructured hexahedron grid of 278,222 cells was used in this

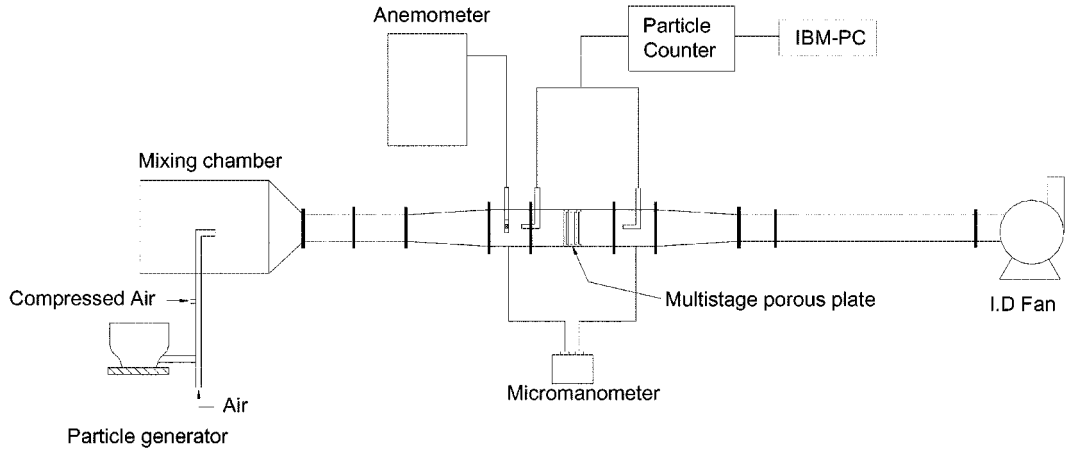

Fig. 1. Experimental apparatus of multi-stage porous plate system.

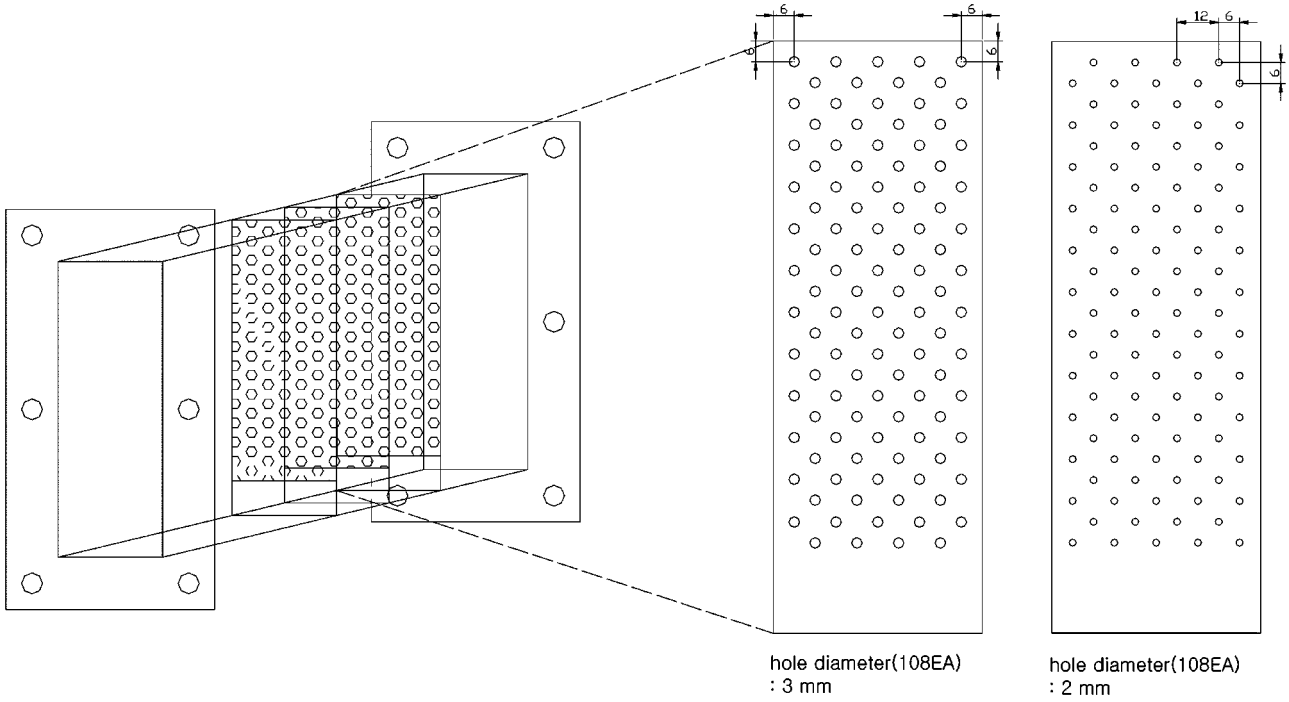

Fig. 2. Configuration of multi-stage porous plate.

Table 1. Hole velocity with hole diameter

Hole diameter (mm)	Porosity (%)	Hole velocity (m/s)	
		$v_{s,in}$=1.0 m/s	$v_{s,in}$=1.2 m/s
2	17.5	30.1	36.1
3	39.3	13.4	16.0

simulation.

2-1. Equation of Gaseous Phase

The governing equations of gas-phase are based on a dilute gas-particle flow. The gas-phase velocity is assumed to be not altered by the particulate flow because of low particle mass loading. To evaluate the turbulent flow, the k-ε model is used in this study.

· Continuity equation

$$\frac{\partial \rho}{\partial t}+\frac{\partial}{\partial x_i}(\rho u_i)=0 \tag{1}$$

· Momentum equation

$$\frac{\partial}{\partial t}(\rho u_i)+\frac{\partial}{\partial x_j}(\rho u_i u_j)=-\frac{\partial p}{\partial x_i}+\frac{\partial \tau_{ij}}{\partial x_j}+\rho g_i+F_i \tag{2}$$

where, p is static pressure and τ_{ij} is stress tensor. ρg_i and F_i are gravity and external force, respectively.

Stress tensor τ_{ij} is given by

$$\tau_{ij}=\left[\mu\left(\frac{\partial u_i}{\partial x_j}+\frac{\partial u_j}{\partial x_i}\right)\right]-\frac{2}{3}\mu\frac{\partial u_l}{\partial x_l}\delta_{ij} \tag{3}$$

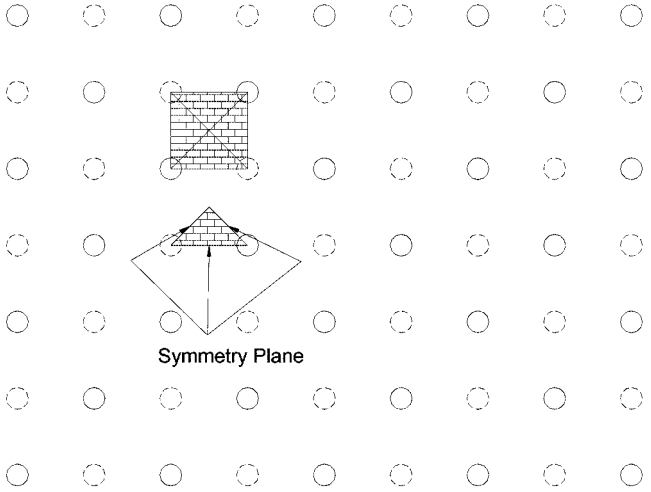

Fig. 3. Computational domain of multi-stage porous plate.

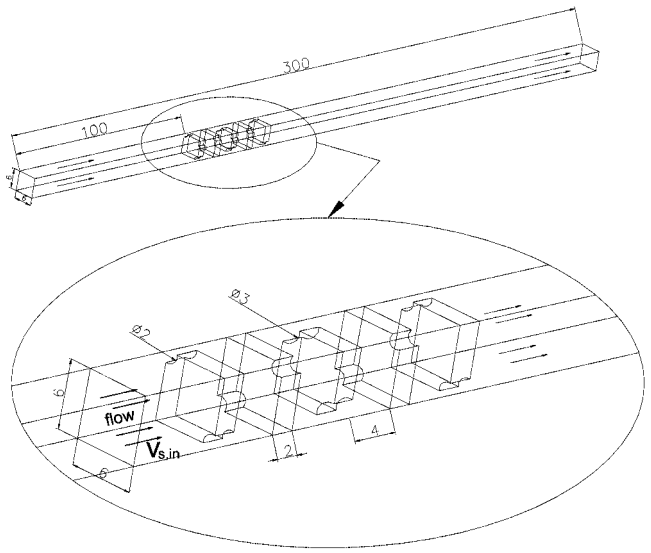

Fig. 4. Numerical model for 5 stage porous plate system (plate interval: 4 mm, plate arrangement: [2, 2, 3, 2, 2 mm]).

The equations of turbulence kinetic energy, k and turbulence energy dissipation rate, ε are given by

$$\rho\frac{Dk}{Dt}=\frac{\partial}{\partial x_i}\left[\left(\mu+\frac{\mu_t}{\sigma_k}\right)\frac{\partial k}{\partial x_i}\right]+G_k-\rho\varepsilon \tag{4}$$

$$\rho\frac{D\varepsilon}{Dt}=\frac{\partial}{\partial x_i}\left[\left(\mu+\frac{\mu_t}{\sigma_\varepsilon}\right)\frac{\partial \varepsilon}{\partial x_i}\right]+C_{1\varepsilon}\frac{\varepsilon}{k}G_k-C_{2\varepsilon}\rho\frac{\varepsilon^2}{k} \tag{5}$$

G_k for the production of turbulence energy by mean velocity gradient, is expressed as

$$G_k=-\rho\overline{u_i'u_j'}\frac{\partial u_j}{\partial x_i} \tag{6}$$

Turbulent viscosity,

$$\mu_t=\rho C_\mu\frac{k^2}{\varepsilon} \tag{7}$$

The model constants C_μ, $C_{1\varepsilon}$, $C_{2\varepsilon}$, σ_k and σ_ε have the following values (Table 2) [Launder et al., 1979].

Table 2. Values of turbulent coefficients

C_μ	$C_{1\varepsilon}$	$C_{2\varepsilon}$	σ_k	σ_ε
0.09	1.44	1.92	1.0	1.3

The dispersion of small particles is strongly affected by the instantaneous fluctuation velocity. The turbulent fluctuation is a random function of space and time. Here, the Continuous Filter White Noise (CFWN) model described by Thomson is used to estimate the instantaneous fluctuation velocity, Accordingly, the ith component of instantaneous fluid velocity satisfies the following stochastic equation:

$$\frac{du_i}{dt}=-\frac{u_i-\overline{u_i}}{T_I}+\left(\frac{2\overline{u_i'^2}}{T_I}\right)\zeta_i(t) \tag{8}$$

Where, $u_i=\overline{u_i}+u_i'$ is an instantaneous fluid velocity and u_i' is the fluctuation velocity.

In Eq. (8), T_I is the particle integral time, which is the average time in turbulent eddies along the particle path. For small particles, the particle integral time may be approximated by Lagrangian integral time T_L. T_L is related to the fluctuation kinetic energy and dissipation rate.

$$T_I\approx T_L\approx 0.15\frac{k}{\varepsilon} \tag{9}$$

In Eq. (8), $\zeta_i(t)$ is a Gaussian vector white noise random process with spectral intensity. And the amplitude of $\zeta_i(t)$ at each time step is given as

$$\zeta_i(t)=\frac{G_i}{\sqrt{\Delta t}} \tag{10}$$

Where, G_i is a Gaussian random number and Δt is the time step used in the simulation.

2-2. Equation of Particulate Phase

For a particle phase, the present study neglects the interaction between suspended particles and particle coagulation owing to the low particle mass loading. To analyze the motion of particles suspended in a gaseous medium, the effects of drag force, turbulent diffusion, Brownian diffusion and electric force are considered for the numerical simulation.

· Equation of particle motion

$$\frac{du_i^p}{dt}=\frac{3\nu C_D Re_p}{4d_p^2 SC_c}(u_i-u_i^p)+n_i(t)+\frac{F_e}{m_p} \tag{11}$$

$$\frac{dx_i}{dt}=u_i^p \tag{12}$$

Where, u_i^p is the velocity of the particle and x_i is its position. S is the ratio of particle density to gas density. $n_i(t)$ is Brownian force per unit mass. m_p is the mass of the particle, and F_e is the electrostatic force.

$$C_D=\frac{24}{Re_p},\quad \text{for } Re_p<1 \tag{13}$$

$$C_D=\frac{24}{Re_p}\left(1+\frac{1}{6}Re_p^{2/3}\right),\quad \text{for } 1<Re_p<400 \tag{14}$$

where, Re_p is the particle Reynolds number defined as

$$Re_p = \frac{d|u_j - u_j^p|}{\nu} \quad (15)$$

In Eq. (11), C_c is the Stokes-Cunningham slip correction factor

The Brownian force per unit mass is modeled as a Gaussian white noise random process.

$$n_i(t) = G_i\sqrt{\frac{\pi S_o}{\Delta t}} \quad (16)$$

The spectral intensity S_o is given by

$$S_o = \frac{216\nu kT}{\pi^2 \rho d_p^5 S^2 C_c} \quad (17)$$

Where, T is the fluid absolute temperature, and ρ is the fluid density. $k=1.38\times10^{-23}$ J/K is the Boltzmann constant.

The third term F_e on the RHS of Eq. (11) is the electrostatic force per unit mass.

$$F_e = qE - \frac{q^2}{16\pi\varepsilon_o y^2} \quad (18)$$

Where, $\varepsilon_o=8.859\times10^{-12}$ As/V is the permittivity of air, and E is the electric field strength. y is the distance from the wall to the particle. The first term of RHS in Eq. (18) is the Coulomb force by the electric field around the particle. The second term is the image force by the virtual electric charge −q. Li and Ahmadi [1993] show that the Coulomb force is dominant when external electric force exists, while image force is effective only for a very short distance from wall to particle.

RESULT

1. Flow Field of Gas-phase

Fig. 5 shows a velocity distribution of the flow field for 5 stage porous plate system (hole diameter: 2, 2, 3, 2, 2 mm, plate interval 4 mm) at the system inlet velocity $v_{s,in}$=1.0 m/s. Gas flow is rap-

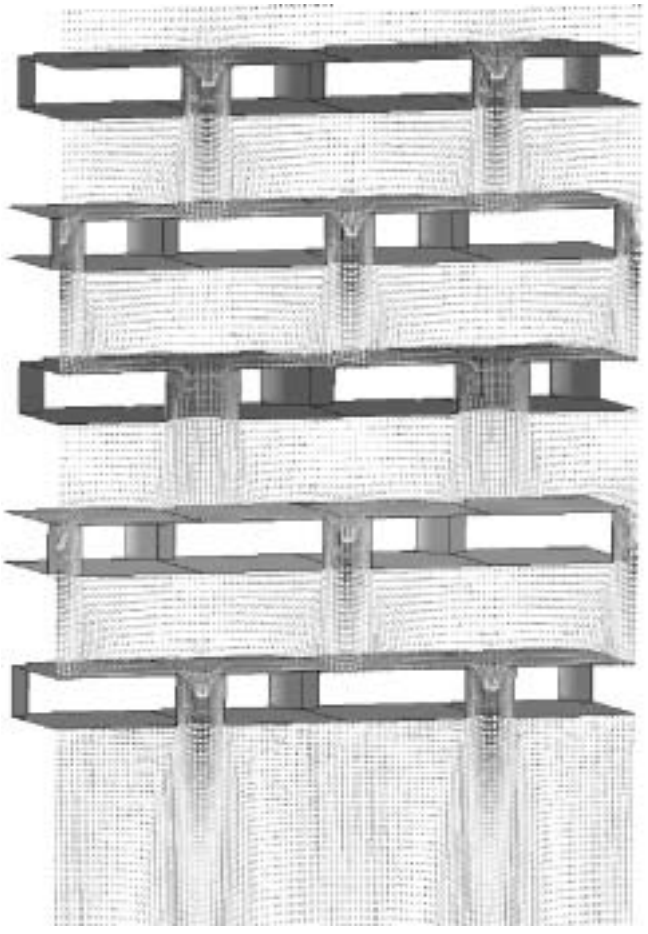

Fig. 5. Velocity vector plot of gas-phase in the multi-stage porous plate system.

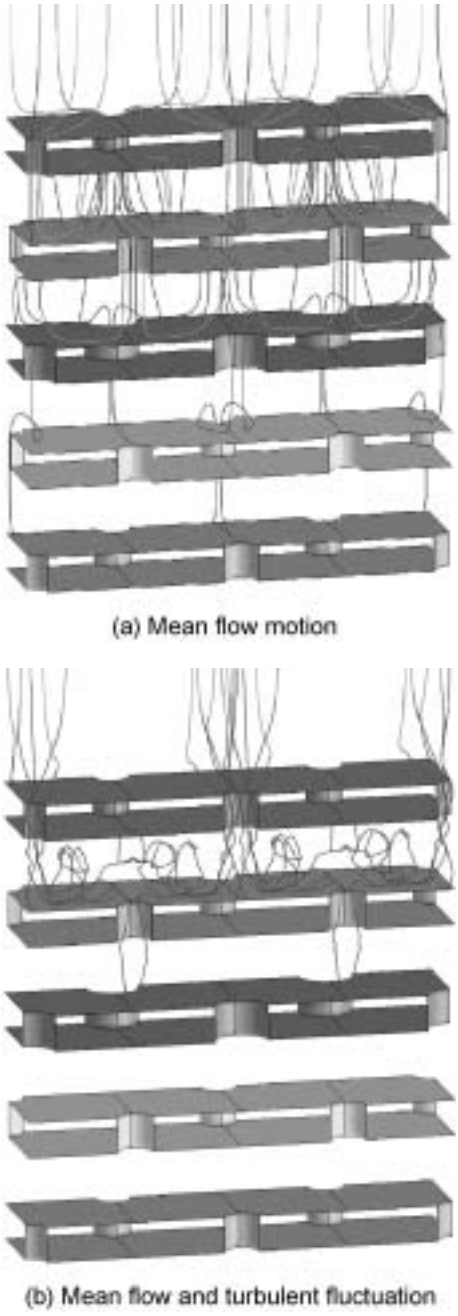

Fig. 6. Particle trajectory of 5 stage system (d_p: 1 μm, $v_{s,in}$: 1.0 m/s, plate arrangement: [2, 2, 3, 2, 2 mm]).

idly accelerated by 31 m/s through the 2 mm diameter holes of the 1st stage porous plate at $v_{s,in}$=1.0 m/s. Gas flows of high velocity that pass through the holes of the 1st stage similar to the stagnation point flow are coming toward the staggered next plate (2nd stage) inducing a strong impaction effect and partially forming a recirculation flow region between two adjacent plates shown in this figure. Such a flow pattern is reproduced iteratively through the 3rd, 4th and next stage.

2. Particle Trajectory

Fig. 6 represents the trajectory of a 1.0 μm diameter particle for the 5 stage system (hole diameter. 2, 2, 3, 2, 2 mm) at a system inlet velocity $v_{s,in}$=1.0 m/s and plate interval, 4 mm. Fig. 6(a) is the result of particle trajectory with consideration of only the drag force by the gaseous mean flow. Particles suspended in a mean flow are accelerated by the rapid carrier gaseous flow passing through the holes of the 1st stage and deposited on the front face of the 2nd stage with a strong impaction effect. This process is generated iteratively with increment of stage number. Fig. 6(b) shows the particle movement by the consideration of turbulent diffusion effect. The particles are separated from the mean flow stream following an eddy motion caused by a strong turbulent fluctuation and then deposited on the front and back face of the 2nd stage and further stages. This phenomenon is more effective for submicron particles and increases the collection efficiency of the present system.

3. Pressure Drop

Pressure drop is one of the major factors for the system design in addition to a collection efficiency to estimate the characteristics of the present system. The major variables for the analysis of pressure drop can be represented as the jet flow velocity (or hole diameter), hole interval, plate to plate distance, and stage numbers, etc.

The pressure drop is described as the following expression in the multi-stage porous plate system:

$$\Delta P = P_n - P_{n+1} = f(\rho v_i^2, \rho v_o^2, d_1, d_2, \text{etc}) \quad (19)$$

Where, P_n, P_{n+1} are pressures between the front and back plate face, and v_i, v_o are flow velocities through a front stage hole and back stage hole. d_1, d_2 are hole interval and plate to plate distance, respectively.

Fig. 7 shows the experimental and numerical results of pressure drop with the stage number increment (1-5 stage) and plate arrangement for plate interval 4 mm, hole interval 6 mm and hole diameter 2 or 3 mm. In the experimental results, pressure drops become lower as 52, 75 mmH_2O, at the system inlet velocity $v_{s,in}$=1.0, 1.2 m/s for 1 stage system (hole diameter 2 mm), respectively, and increase in relation to the square order of inlet velocity as shown in Eq. (19). For the 2 stage system [2, 2 mm], ΔP at $v_{s,in}$=1.0, 1.2 m/s increases significantly as 123, 183 mmH_2O, respectively, compared to that of 1 stage. It means that the jet velocity (flow velocity passing through the 1st stage hole) toward the 2nd stage is higher than that toward the 1st stage (i.e., flow velocities toward the 1st stage, 2nd stage are 1.0 m/s and 30.1 m/s at $v_{s,in}$=1.0, repectively). For a 3 stage system [2, 2, 3 mm], pressure drops are shown as 152, 221 mmH_2O in the system inlet velocity $v_{s,in}$=1.0, 1.2 m/s and rate of increase of ΔP for 3 stage becomes lower than that of the 2 stage with the stage number increment because the 3rd stage hole diameter increases to 3 mm.

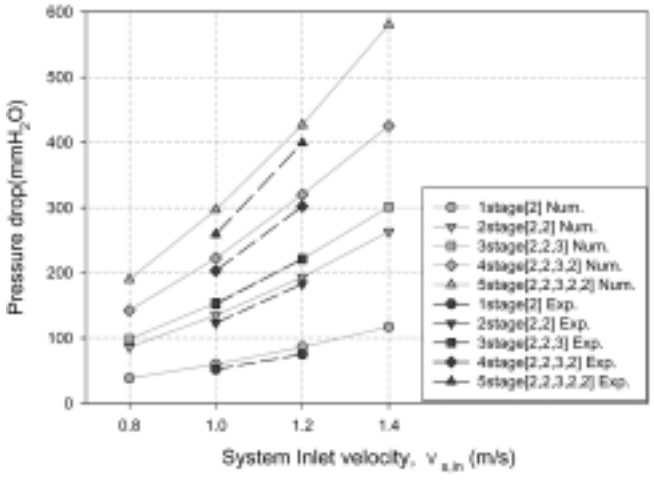

Fig. 7. Pressure drop with stage number (plate interval: 4 mm).

ΔP of 4 stage [2, 2, 3, 2 mm] and 5 stage [2, 2, 3, 2, 2 mm] system are represented as 203, 259 mmH_2O in $v_{s,in}$=1.0 m/s, and 302, 399 mmH_2O in $v_{s,in}$=1.2 m/s, respectively. As the system inlet velocity $v_{s,in}$ increases, ΔP becomes much higher due to the proportionality with the square order of inlet velocity by the Eq. (19).

The numerical results show a similar trend predicting a slightly higher ΔP in comparison with the experimental results because the attenuation of viscosity effect in the laminar sublayer near the porous plate surface by the particles suspended in a gaseous flow is not considered for the present numerical simulation. Thus, it turns out that the pressure drop characteristics with the inlet velocity and stage number can be estimated almost exactly by the numerical simulation for a multi-stage porous plate system.

4. Collection Efficiency

4-1. Fractional Collection Efficiency

To analyze the collection efficiency of the present system, the particle number concentration is estimated at the inlet and outlet of the system, and fractional collection efficiency is obtained by

$$\eta_j(\%) = \frac{N_{in,j} - N_{out,j}}{N_{in,j}} \times 100 \quad (20)$$

Where, η_j is fractional collection efficiency and $N_{in,j}$ is fractional particle number concentration at the inlet. $N_{out,j}$ is fractional particle number concentration at the outlet.

Main collection mechanisms of the present system are considered as impaction (inertial force), turbulent diffusion, Brownian diffusion and electric force. In general, the cut-off diameter $d_{p,cut}$ is expressed as $d_{p,cut} = 9\mu d Stk_{50}/\rho_p v_{in}$ when the impaction effect is applied to the system. To increase the collection efficiency (i.e., decrease of $d_{p,cut}$), a smaller hole diameter and higher jet velocity are required, but they result in the increment of pressure drop, simultaneously. Thus, for an optimal design of the present system, the hole diameter d and system inlet velocity (or jet velocity) $v_{s,in}$, etc. can be treated as the major design parameters. The particle movement governed by the mean flow motion, turbulent fluctuation, Brownian diffusion and electric force is analyzed to estimate the collection efficiency by numerical simulation.

Fig. 8 shows the fractional collection efficiency with the effect of only mean flow motion for a 3 stage system [2, 2, 3 mm] at $v_{s,in}$= 0.8, 1.0, 1.2, 1.4 m/s by the numerical simulation. Collection effi-

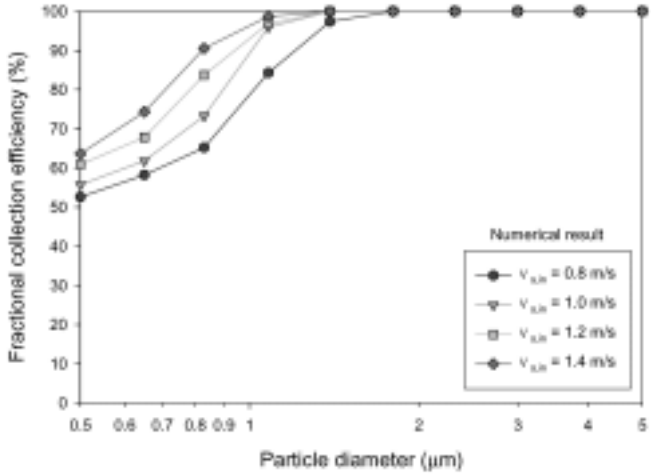

Fig. 8. Fractional collection efficiency of 3 stage system by the effect of only mean flow (plate interval: 4 mm, plate arrangement: [2, 2, 3 mm]).

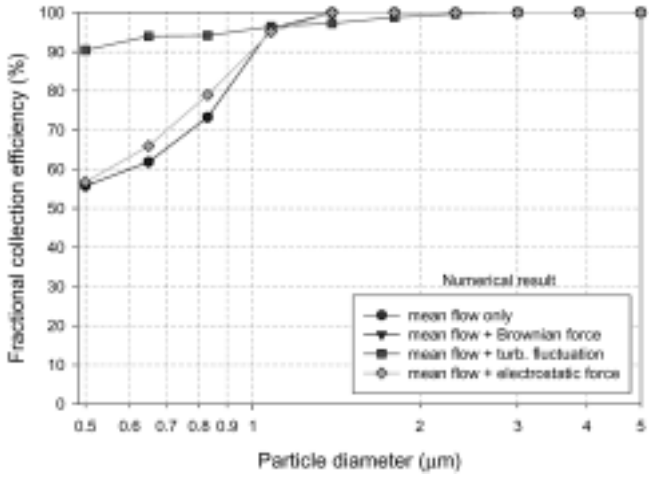

Fig. 10. Fractional collection efficiency of 3 stage system with various collection mechanism ($v_{s,in}$: 1.0 m/s, plate interval: 4 mm, plate arrangement: [2, 2, 3 mm]).

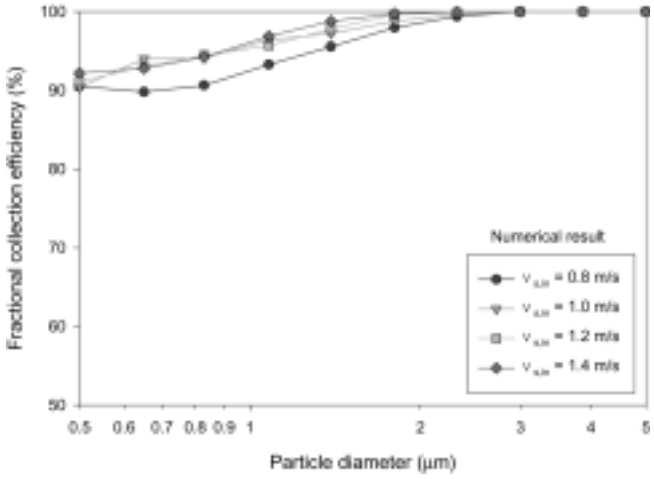

Fig. 9. Fractional collection efficiency of 3 stage system by the effect of mean flow and turbulent fluctuation (plate interval: 4 mm, plate arrangement: [2, 2, 3 mm]).

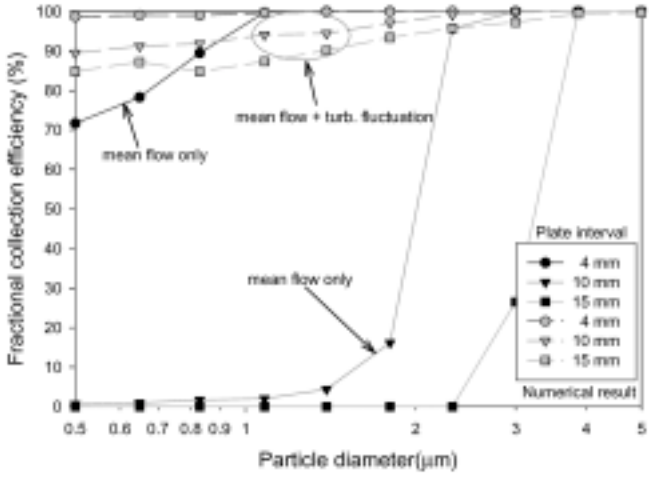

Fig. 11. Fractional collection efficiency of 5 stage system by the effect of mean flow and turbulent fluctuation ($v_{s,in}$: 1.0 m/s, plate arrangement: [2, 2, 3, 2, 2 mm]).

ciency for the particle size range over 1 μm diameter approaches near 100% due to relatively higher inertial force at $v_{s,in}$=1.0, 1.2, 1.4 m/s except for 0.8 m/s, while becomes much lower below 1 μm diameter without considering the diffusion effect as system inlet velocity, $v_{s,in}$ decreases.

As in Fig. 9, considering the turbulent diffusion effect with the mean flow motion at the same simulation condition as that of Fig. 8, higher efficiency over 90% for the submicron particle below 1 μm is estimated due to the effect of strong turbulent fluctuation in spite of lower inertial force (i.e., relatively small particle).

Fig. 10 represents the fractional collection efficiency with the effect of turbulent diffusion, Brownian diffusion and electric force affecting particle movement in addition to mean gaseous flow motion for the 3 stage [2, 2, 3 mm], plate interval 4 mm and $v_{s,in}$=1.0 m/s. As shown in the Figure, the effect of Brownian motion is almost negligible for the given inlet velocity ($v_{s,in}$=1.0 m/s) and particle size range. Applying electric force of uniform electric intensity, 600 kV/m at the precharger in front of 1st stage, the effect of electric force by the only image force without the electric intensity of the 2nd stage is considered from the sufficiently charged particle in the precharger incoming into the 2nd stage. Then, the collection efficiency is improved about 5% for submicron particles below 1 μm by the effect of electric force, while its improvement is relatively negligible for larger particles over 1 μm due to higher inertial force.

Fig. 11 shows the collection efficiency for the 5 stage system [2, 2, 3, 2, 2 mm] and $v_{s,in}$=1.0 m/s with the plate interval 4, 10, 15 mm by the numerical simulation. As the plate interval increases from 4 to 15 mm, the collection efficiency becomes lower since the particles escaping from the collection area following the gaseous streamline increase by the enlargement of particle moving distance to the collection plate with plate interval increment. This phenomenon is significantly shown for submicron particles below 3 μm diameter due to the decrease of inertial force. Moreover, considering the turbulent fluctuation with mean flow motion, the improvement rate of

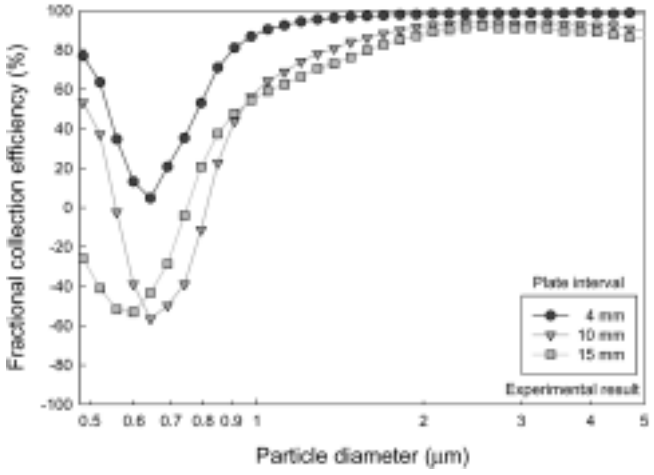

Fig. 12. Fractional collection efficiency with plate interval for 5 stage system ($v_{s,in}$: 1.0 m/s, plate arrangement: [2, 2, 3, 2, 2 mm]).

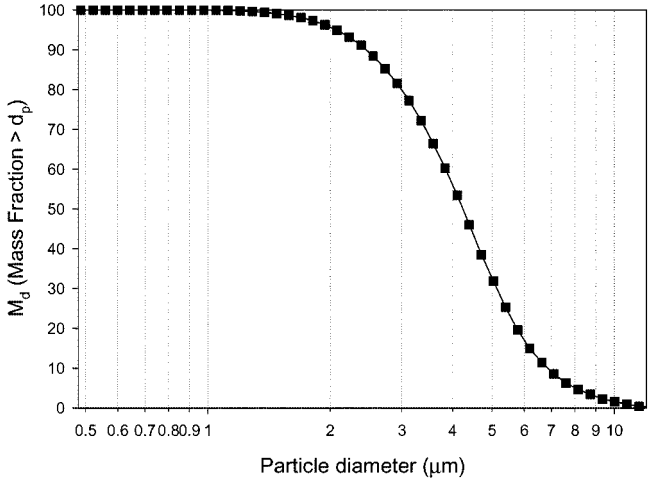

Fig. 13. Plot of M_d vs. d_p of test coal fly ash.

collection efficiency for the submicron particle becomes higher by the enlargement of the turbulent diffusion area as the plate interval increases.

Fig. 12 represents the experimental results of collection efficiency at the same operation condition as that of Fig. 11. The results show that the efficiency similarly decreases with the plate interval increment as predicted in the numerical simulation. Specifically, it is estimated that the collection efficiency is maintained higher than 80% for all the particle size range over 2 μm diameter, while rapidly decreases below 2 μm diameter because of relatively lower particle inertial force. And, minimum efficiency appears around 0.7 μm diameter, but the collection efficiency for smaller particles than 0.7 μm increases by the increment of turbulent diffusion effect. The negative (−) sign of collection efficiency represents that the numbers of submicron particles at system exit are in excess of those at system inlet due to the particle disintegration phenomenon.

4-2. Overall Collection Efficiency

The overall collection efficiency characteristics are analyzed by the experimental and numerical simulation with various parameters such as system inlet velocity, hole diameter, stage number and plate interval, etc. The overall collection efficiency, η_t is expressed as

$$\eta_t(\%) = \frac{\sum(V_j N_{in,j} - V_j N_{out,j})}{\sum(V_j N_{in,j})} \times 100 \quad (21)$$

Where, V_j is the volume of each particle diameter. $N_{in,j}$ is the number of influent particles per each diameter and $N_{out,j}$ is the number of effluent particles per each diameter.

The Rosin-Rammler distribution can be defined as the exponential relationship between the particle diameter d_p, and the mass fraction of particles with diameter greater than d_p, M_d.

$$M_d = \exp(-(d_p/\overline{d_p})^n) \quad (22)$$

Where, $\overline{d_p}$ is the mean diameter and n is the spread parameter.

Fig. 13 represents the Rosin-Rammler distribution of coal fly ash used in the present numerical simulation. In this Figure, $\overline{d_p}$ and n are 1.22 μm, 0.407, respectively.

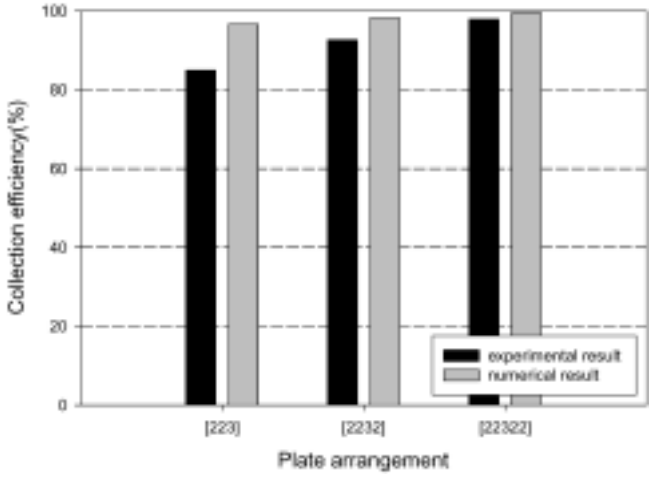

Fig. 14. Overall collection efficiency with stage number ($v_{s,in}$: 1.0 m/s, plate interval: 4 mm).

Fig. 14 means the overall collection efficiency with stage number (plate arrangement) for $v_{s,in}$=1.0 m/s and plate interval 4 mm. Numerical results of overall efficiency are shown higher as 96.7, 98.2, 99.5% for the 3 stage [2, 2, 3 mm], 4 stage [2, 2, 3, 2 mm], 5 stage [2, 2, 3, 2, 2 mm] system with increment of stage number, respectively. And the experimental results show a similar trend to those of numerical simulation as 84.9, 92.6, 97.9% efficiency. It means a little lower efficiency than that of numerical result due to the rescattering effect of particles deposited on the collection plate. Fig. 15 represents the overall collection efficiency with the plate interval 4, 10, 15 mm for the 5 stage system [2, 2, 3, 2, 2 mm] and $v_{s,in}$=1.0 m/s, by the numerical and experimental method. In case of the mean gaseous flow motion for the particle movement, the overall efficiencies with the plate interval 4, 10, 15 mm become relatively low as 93.8, 47.2, 32.6%, respectively.

However, considering the turbulent diffusion effect with the mean flow motion, collection efficiencies are shown quite high as 99.5, 96.0, 92.8% with the plate interval (4, 10, 15 mm), as stated earlier in the section on fractional collection efficiency. There is a slight difference between the numerical and experimental results show-

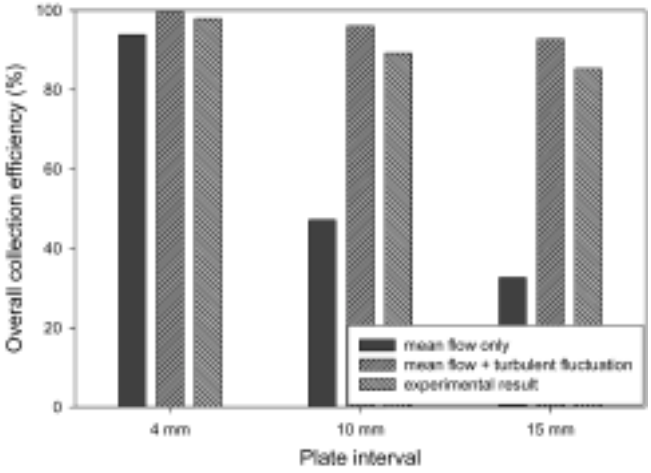

Fig. 15. Overall collection efficiency of 5 stage system ($v_{s,in}$: 1.0 m/s, plate interval: 4, 10, 15 mm, plate arrangement: [2, 2, 3, 2, 2 mm]).

ing a little lower efficiency in the experiment than that of numerical simulation due to the particle rescattering effect in the case of the experiment.

CONCLUSIONS

The characteristics of collection efficiency and pressure drop for the multi-stage porous system were evaluated by experiment and numerical simulation with the operation parameters such as the stage number, plate interval, hole diameter and system inlet velocity, etc. In the numerical simulation, the effect of major factors such as mean flow motion, turbulent fluctuation, Brownian motion and electric force upon the particle movement was analyzed for the collection efficiency of the present system. The following conclusions are summarized.

1. Pressure drop highly increases with increment of stage number (1-5 stage) and system inlet velocity. In particular, ΔP of the 5 stage system [2, 2, 3, 2, 2 mm] at $v_{s,in}$=1.0, 1.2 m/s is shown as 296, 428 mmH_2O by the numerical simulation and 259, 399 mmH_2O in the experiment.
2. The effect of major parameters such as mean flow motion, turbulent fluctuation, Brownian motion and electric force on the particle movement was evaluated numerically, and collection efficiency for the submicron particle below 1 μm was highly improved due to a turbulent diffusion effect.
3. Overall collection efficiencies with increment of stage number (3-5 stage) become higher as 96.7, 98.2, 99.5% at the plate interval 4 mm and $v_{s,in}$=1.0 m/s by the numerical simulation and 84.9, 92.6, 97.9% in the experiment, respectively.
4. For the 5 stage system [2, 2, 3, 2, 2 mm] and $v_{s,in}$=1.0 m/s, overall collection efficiencies with plate interval of 4, 10, 15 mm are estimated as 99.5, 96.0, 92.8% computationally and 97.9, 89.2, 85.3% showing slightly lower efficiency compared to the numerical results due to the particle rescattering effect, experimentally.
5. It is necessary to evaluate the optimal design parameters such as stage number, plate arrangement, plate interval, plate porosity and system inlet velocity, etc. for the analysis of collection efficiency and pressure drop of multi-stage porous plate system.

ACKNOWLEDGMENT

This work was supported by energy & resource technology development project (2002-E-ID03-P-02-0-000) of Korea Energy Management Corporation.

NOMENCLATURE

C_c : stokes-Cunningham slip correction factor
d_p : particle diameter
E : electric field strength
F : external force
F_e : electrostatic force
G_k : production of turbulence energy by mean velocity gradient
G_i : gaussian random number
k : turbulence kinetic energy
M_d : mass fraction of particles with diameter greater than d_p
m_p : mass of the particle
$n_i(t)$: Brownian force per unit mass
p : static pressure
Re_p : particle Reynolds number
S : ratio of particle density to gas density
S_o : spectral intensity
T_I : particle integral time
T_L : Lagrangian integral time
u_i : velocity of gas
u_i^p : velocity of particle
$v_{s,in}$: system inlet velocity
x_i : position of particle
y : distance from the wall to the particle

Greek Letters

ε : turbulence energy dissipation rate
η_t : overall collection efficiency
$\zeta_i(t)$: Gaussian vector white noise random process with spectral intensity
τ_{ij} : stress tensor

REFERENCES

Benjamin, J. and Wang, H. C., "On the Shape of Impactor Efficiency Curves," *J. Aerosol Sci*., **26**, 1139 (1995).

Bernard, A. O., Virgil, A. M., Jolyon, P. M. and Mark, W. N., "Development and Calibration of a Low-Flow Version of the Marple-Miller Impactor (MMITM)," *Aerosol Sci. Tech*., **29**, 307 (1998).

Chang, M. C., Kim, S. H. and Constantinos, S., "Experimental Studies on Particle Impaction and Bounce: Effects of Substrate Design and Material," *Atmospheric Environment*, **33**, 2313 (1999).

Choi, H.-K., Park, S.-J., Lim, J.-H., Kim, S.-D., Park, H.-S. and Park, Y.-O., "A Study on the Characteristics of Improvement in Filtration Performance by Dust Precharging," *Korean J. Chem. Eng.*, **19**, 342 (2002).

Daniel, J. R. and Anthony, S. G., "Showerhead-enhanced Inertial Particle Deposition in Parallel Plate Reactors," *Aerosol Sci. Tech*., **28**, 105

(1998).
Frederick, E. R., "How Dust Filter Selection Depends on Electrostatics," *Chemical Engineering*, **68**, 107 (1961).
Launder, B. E. and Spalding, D. B., "Lectures in Mathematical Models of Turbulence," Academic Press, 98 (1979).
Lee, J. E. and Lee, J. K., "Effect of Microbubbles and Particle Size on the Particle Collection in the Column Flotation," *Korean J. Chem. Eng.*, **19**, 703 (2002).
Lee, J. K. and Shin, J. H., "Design and Performance Evaluation of Triboelectrostatic Separation System for the Separation of PVC and PET Materials using a Fluidized Bed Tribocharger," *Korean J. Chem. Eng.*, **20**, 572 (2003).
Miles, L. C., "Filter Dust Collectors - Design and Application," McGraw-Hill, Inc. (1994).
Novick, V. J. and Alvalez, J. L., "Design of a Multistage Virtual Impactor," *Aerosol Sci. Tech*., **6**, 63 (1987).
Oglesby, S. and Nichols, G. B., "Electrostatic Precipitation Technology," Marcel Dekker Inc. New York (1978).
Ohtsuka, K. and Shimoda, M., "Mechanism of Fabric Filtration by Electrostatic Augmentation," *Journal of Electrostatics*, **18**, 93 (1986).
Park, Y. O., Park, H. S., Park, S. J., Kim. S.- D., Choi, H. K. and Lim, J. H., "Development and Evaluation of Multilayer Air Filter Media," *Korean J. Chem. Eng.*, **18**, 1020 (2001).
Robinson, M., "Electrostatic Precipitation in Air Pollution Controled," W. Strauss, part 1, Wiley-Interscience, New York (1971).
Yoa, S. J., Cho, Y. S., Choi, Y. S. and Baek, J. H., "Characteristics of Electrostatic Cyclone/Bag Filter with Inlet Types (Lab And Pilot Scale)," *Korean J. Chem. Eng.*, **18**, 539 (2001).